

RSC Advances



This is an *Accepted Manuscript*, which has been through the Royal Society of Chemistry peer review process and has been accepted for publication.

Accepted Manuscripts are published online shortly after acceptance, before technical editing, formatting and proof reading. Using this free service, authors can make their results available to the community, in citable form, before we publish the edited article. This *Accepted Manuscript* will be replaced by the edited, formatted and paginated article as soon as this is available.

You can find more information about *Accepted Manuscripts* in the [Information for Authors](#).

Please note that technical editing may introduce minor changes to the text and/or graphics, which may alter content. The journal's standard [Terms & Conditions](#) and the [Ethical guidelines](#) still apply. In no event shall the Royal Society of Chemistry be held responsible for any errors or omissions in this *Accepted Manuscript* or any consequences arising from the use of any information it contains.

ARTICLE

Hexanuclear [Ni₂Ln₄] clusters exhibiting enhanced magnetocaloric effect and slow magnetic relaxation

Cite this: DOI: 10.1039/x0xx00000x

Cai-Ming Liu,^{*a} De-Qing Zhang^a and Dao-Ben Zhu^a

Received 00th January 2012,

Accepted 00th January 2012

DOI: 10.1039/x0xx00000x

www.rsc.org/

Two hexanuclear 3d-4f cluster complexes containing the pyridine-2-aldoximate ligand (pao⁻), [Ni₂Ln₄(hfac)₈(pao)₆(CH₃COO)₂(MeOH)]·H₂O·MeOH (Ln = Gd, **1**; Ln = Dy, **2**; hfac⁻ = hexafluoroacetylacetonate), have been synthesized, which show similar structures with an interesting 'trigonal bipyramid' metal topology. Magnetic determinations revealed that the Ni-Gd specie has a spin ground state of 16 due to the dominant ferromagnetic exchange, exhibiting an enhanced magnetocaloric effect, which can be used as the cryogenic magnetic cooler; while the Ni-Dy analogue displays slow magnetic relaxation, typical character for a single-molecule magnet.

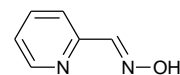
Introduction

Recently, heterometallic 3d-4f cluster complexes have played an important role in the development of nanoscale molecular magnetic materials, especially for single-molecule magnets (SMMs)¹ and low-temperature magnetic coolers.² The SMMs possess many potential applications in fields such as quantum computing, magnetic information storage devices and spintronics,^{1,3} because they display slow magnetization relaxation and superparamagnet-like behaviors at low temperature. While the environmentally friendly low-temperature magnetic coolers are based on magnetocaloric effect (MCE), which is commonly evaluated by magnetic entropy change ($-\Delta S_m$).^{2,4} Interestingly, both the molecular magnetic materials require high spin ground states, which can be achieved by the ferromagnetic interaction between the 3d and 4f metal ions. Furthermore, the magneto-anisotropy is necessary for the SMMs whereas the magneto-isotropy favors the MCEs, therefore, it supplies a practical approach to the different nano-sized molecular magnetic materials, either the SMM or the low-temperature magnetic cooler, through change of the Ln³⁺ ions with different magneto-isotropy in the same 3d-4f cluster family. For examples, the Dy³⁺ ion is often used for the design of the SMMs, while the Gd³⁺ ion is an excellent element to construct molecular magnetic coolers.

Up to now, more and more heterometallic Ni-Gd clusters have been designed to be low-temperature magnetic coolers,⁵ including very large nuclearity aggregates [Ni₉Gd₂],^{5a} [Ni₁₂Gd₃],^{5d} [Ni₁₀Gd₄₂]^{5c} and [Ni₁₂Gd₃₆].^{5b} However, still no enhanced MCEs were observed in these compounds. In addition, their Ni-Dy analogues seldom show slow magnetization relaxation, the main reason maybe is that the whole molecule's magneto-anisotropy of the heterometallic 3d-4f clusters is difficult to be controlled to display the SMM properties. Therefore, it is necessary to further design and synthesize new 3d-4f cluster family in which a switch from the SMM to the coolant (or vice versa) can be achieved via facile lanthanide ion changes. For the Ni-Ln cluster complexes, only two such systems have been reported recently.^{5c,5i}

We are also interested in the molecular nanomagnet materials.⁶ Recently, we used a salicylaldoximate ligand (Et-sao²⁻) to construct a heptanuclear Mn-Ln cluster system

Mn^{III}₃Mn^{IV}O₃Ln₃(OH)(piv)₆(EtO)₃(EtOH)₃(Et-sao)₃ (Ln = Gd and Dy; piv = pivalate), whose magnetic properties could be adjusted to be the SMM or the cryogenic magnetic cooler, depending on the lanthanide ions used.⁷ As a continuation of the work, we chose another oxime ligand, pyridine-2-aldoximate (pao⁻, Scheme 1), to assemble the 3d-4f cluster system. Herein, we report the syntheses, crystal structures and magnetic properties of two novel hexanuclear Ni-Ln cluster complexes, [Ni₂Ln₄(hfac)₈(pao)₆(CH₃COO)₂(MeOH)]·H₂O·MeOH (Ln = Gd, **1**; Ln = Dy, **2**; hfac⁻ = hexafluoroacetylacetonate), which show a 'trigonal bipyramid' metal topology and ferromagnetic interactions. Interestingly, complex **1** displays an enhanced MCE while **2** shows slow magnetic relaxation.



Scheme 1. paoH ligand

Experimental

Materials and physical measurements

Unless otherwise mentioned, all reagents were commercially available and used as received. The starting materials Ni(paoH)₂Cl₂ and Ln(acac)₂(CH₃COO)(H₂O)₂ were prepared according to the literature methods.^{8,9} Elemental analyses were performed on a Varlo ELIII elemental analyzer. Infrared spectra were recorded on a TENSOR27 Bruker spectrophotometer in the region of 400–4000 cm⁻¹ using the KBr pallet samples. The magnetic susceptibility measurements were carried out on a Quantum Design MPMS-XL5 SQUID magnetometer in the temperature range of 1.9–300 K. Diamagnetic corrections of all constituent atoms were estimated from Pascal's constants.¹⁰

Preparation of 1

A mixture of Ni(paoH)₂Cl₂ (0.25 mmol), Gd(acac)₂(CH₃COO)(H₂O)₂ (0.25 mmol) and Et₃N (0.5 mmol) in 10 ml of MeOH was sonicated for 10 min, a brown solution was formed, which was allowed to slowly evaporate for several days, giving brown block crystals. Yield 70% based on Gd. Elemental analysis (%) calculated for C₈₂H₅₄Gd₄F₄₈N₁₂Ni₂O₂₉: C, 29.58; H, 1.63; N, 5.05; Found: C, 29.53; H, 1.67; N, 5.01. IR (KBr, cm⁻¹): 3429(b, s), 3140(w), 3072(w), 1655(s), 1608(m), 1580(m), 1555(m), 1530(s), 1511(m), 1478(m), 1443(w), 1415(w), 1347(w), 1256(s), 1208(s), 1142(s), 1099(m), 1017(w), 950(w), 917(w), 891(w), 795(m), 774(w), 749(w), 680(w), 661(m), 642(w), 585(m), 528(w), 447(w), 422(w).

Preparation of 2

Complex **2** was produced as brown block crystals by an approach similar to that of **1**, except that Dy(acac)₂(CH₃COO)(H₂O)₂ was used instead of Gd(acac)₂(CH₃COO)(H₂O)₂. Yield 65% based on Dy. Elemental analysis (%) calculated for C₈₂H₅₄Dy₄F₄₈N₁₂Ni₂O₂₉: C, 29.39; H, 1.62; N, 5.02; Found: C, 29.43; H, 1.65; N, 4.99. IR (KBr, cm⁻¹): 3444(b, s), 3141(w), 3075(w), 1654(s), 1608(m), 1580(m), 1555(m), 1531(s), 1511(m), 1478(m), 1444(w), 1419(w), 1386(w), 1346(w), 1257(s), 1208(s), 1144(s), 1099(m), 1017(w), 951(w), 921(w), 891(w), 797(m), 775(w), 749(w), 681(w), 662(m), 642(w), 586(m), 528(w), 447(w), 422(w).

X-ray crystallography

The diffraction data were collected at 173(2) K on a Rigaku Saturn 724 diffractometer with monochromated Mo-K α radiation ($\lambda = 0.71073$ Å). Lorentz-polarization effects and absorption corrections were applied. Direct methods were adopted to solve the structures, which were refined with full-matrix least-squares techniques using *SHELXS-97* and *SHELXL-97* programs.¹¹ The non-hydrogen atoms were refined anisotropically, and the hydrogen atoms were added theoretically onto the attached atoms and refined isotropically with fixed thermal factors. Selected crystallographic data and structure determination parameters are given in Table 1.

Table 1. Crystal data and structural refinement parameters for **1** and **2**.

Compound	1	2
Chemical formula	C ₈₂ H ₅₄ Gd ₄ F ₄₈ N ₁₂ Ni ₂ O ₂₉	C ₈₂ H ₅₄ Dy ₄ F ₄₈ N ₁₂ Ni ₂ O ₂₉
Formula weight	3329.79	3350.79
Crystal system	Monoclinic	Monoclinic
Space group	<i>P2₁/c</i>	<i>P2₁/c</i>
<i>a</i> /Å	16.176(3)	16.217(3)
<i>b</i> /Å	25.626(5)	25.446(5)
<i>c</i> /Å	28.494(6)	28.525(6)
β /°	103.74(3)	104.02(3)
<i>V</i> /Å ³	11474(4)	11421(4)
<i>Z</i>	4	4
<i>T</i> /K	173 (2)	173 (2)
λ (Mo-K α)/Å	0.71073	0.71073
ρ_{calc} /g · cm ⁻³	1.928	1.949
μ (Mo-K α)/mm ⁻¹	2.753	3.060
θ range	1.08° ≤ θ ≤ 25.02°	1.09° ≤ θ ≤ 25.02°
Limiting indices	-18 ≤ <i>h</i> ≤ 19, -30 ≤ <i>k</i> ≤ 30, -33 ≤ <i>l</i> ≤ 33	-19 ≤ <i>h</i> ≤ 19, -30 ≤ <i>k</i> ≤ 30, -33 ≤ <i>l</i> ≤ 33
Reflections collected	64729	68739
Unique reflections	20141	20030
<i>R_i</i> ^a [<i>I</i> > 2 σ (<i>I</i>)]	0.0741	0.0703
<i>wR₂</i> ^b [<i>I</i> > 2 σ (<i>I</i>)]	0.1514	0.1432

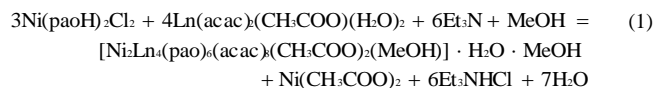
<i>R_i</i> ^a [all data]	0.0869	0.0821
<i>wR₂</i> ^b [all data]	0.1583	0.1493
<i>S</i> [<i>I</i> > 2 σ (<i>I</i>)]	1.156	1.156
<i>S</i> [all data]	1.160	1.156

$$^a R_i = \sum |F_o| - |F_c| / \sum |F_o|, ^b wR_2 = \sum \{ [w(F_o^2 - F_c^2)^2] / \sum [wF_o^2] \}^{1/2}$$

Results and discussion

Synthesis

It is well known that the polydentate ligand salicylaldehyde (R-saoH₂, R = H, Me, Et, Ph etc.) has been extensively employed to synthesize a series of [Mn₃] and [Mn₆] SMMs.¹² Furthermore, the ligand pyridine-2-aldoxime has been utilized to construct several heterometallic polynuclear cluster complexes recently. For examples, Christou et al assembled an unusual Ni₈Dy₈ 'core-shell' complex using the pyridine-2-aldoxime directly;¹³ while the Miyasaka group and the Chen group employed 'metal oximate' [Ni(pao)₂(py)₂] and [Ni(paoH)₂Cl₂] as the starting materials to construct several heterometallic polynuclear Ni-Mn clusters, respectively.¹⁴ On the other hand, the starting materials Ln(acac)₂(CH₃COO)(H₂O)₂ have been explored to construct the cluster complexes with three types of bridging organic ligands, which include the acetate ligand, the hfac⁻ ligand and the third bridging ligand.⁹ In order to obtain **1** and **2** in a simple way, we also adopted the strategy of using the 'metal oximates' as ligands, and Ln(acac)₂(CH₃COO)(H₂O)₂ were used as another starting materials. When Ni(paoH)₂Cl₂ was treated with Ln(acac)₂(CH₃COO)(H₂O)₂ in methanol in the presence of Et₃N, **1** and **2** could be produced easily. Obviously, Ln(acac)₂(CH₃COO)(H₂O)₂ provided the basic conditions to facilitate deprotonation of the oxime. The preparation of **1** and **2** can be represented by eqn (1).



The two 'one-pot' reactions are simple, but yields good.

Crystal structures

Both complexes crystallize in the space group *P2₁/c*. As shown in Fig. 1, the hexanuclear metal core of **1** can be described as a distorted trigonal bipyramid but some edges are fictitious, in which the [Gd₄] triangle plane possesses three Gd³⁺ ions at the corners and one central Gd³⁺ ion lying 0.5942 Å above the plane; while two Ni²⁺ ions occupy the apical sites. There are two types of peripheral Gd³⁺ ions according to the coordination modes: the Gd2 and Gd4 atoms have a nearly monocapped square-antiprism environment (Fig. S1), completed by six oxygen atoms from three hfac⁻ ligands, two oximate oxygen atoms from two Ni(pao)₃⁻ building blocks, and one oxygen atom from the $\eta^1:\eta^2:\mu_3\text{-AcO}^-$ ligand (for Gd4) or the $\eta^2:\eta^2:\mu_4\text{-AcO}^-$ ligand (for Gd2); whereas the Gd3 atom shows a distorted square-antiprism coordinate geometry (Fig. S1), bonded by four oxygen atoms from two hfac⁻ ligands, one oxygen atom from the $\eta^1:\eta^2:\mu_3\text{-AcO}^-$ ligand, one oxygen atom from the $\eta^2:\eta^2:\mu_4\text{-AcO}^-$ ligand, and one oxygen atom from the terminal methanol molecule. The centered Gd1 atom also exhibits a distorted monocapped square-antiprism configuration (Fig. S1), but coordinated by six oximate oxygen atoms from two Ni(pao)₃⁻ building blocks, two oxygen atoms from the $\eta^2:\eta^2:\mu_4\text{-AcO}^-$ ligand, and one oxygen atom from the $\eta^1:\eta^2:\mu_3\text{-}$

AcO⁻ ligand. The Gd-O bond lengths of the eight-coordinate Gd3 atom (average value of 2.375 Å) are obviously smaller than those for the nine-coordinate Gd atoms (mean values of 2.477, 2.429 and 2.442 Å for the Gd1, Gd2 and Gd4 atoms, respectively).

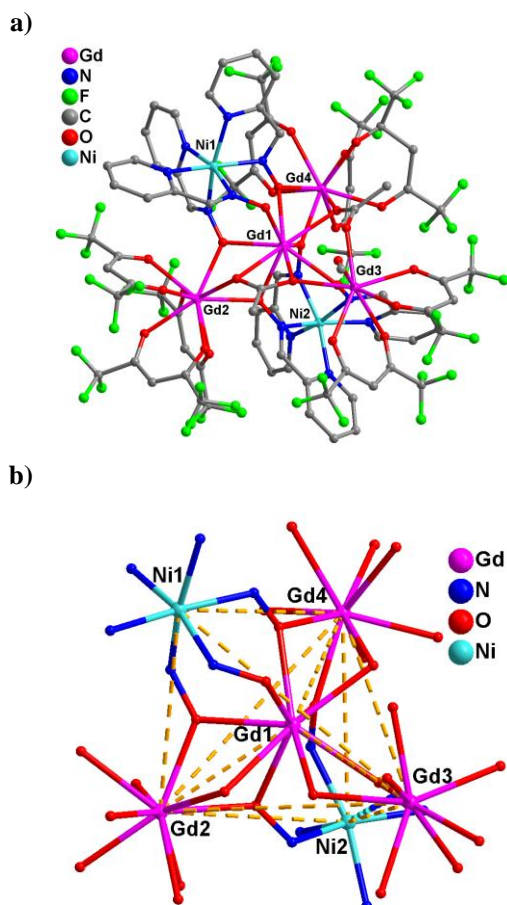


Fig. 1. Crystal structure of **1**, all H atoms and solvent molecules are omitted for clarity (a), and the coordination environments of the Gd and Ni atoms, the dotted lines describe the trigonal bipyramid metal topology (b).

There are two crystallographically independent nickel atoms, each of which is bonded by three pao⁻ ligands in a perpendicular way, exhibiting a distorted [NiN₆] octahedron geometry. The Ni-N bond distances for the Ni1 atom (average 2.068 Å) are very close to those for the Ni2 atom (2.069 Å). Interestingly, all three oximate groups of the Ni(pao)₃⁻ building block are situated at the same side in order to bond the central Gd1 atom, acting as a tridentate ‘metal oximate’ ligand. Besides, three oximate oxygen atoms from three pao⁻ ligands of the Ni1 atom further cement the [Gd₄] triangle plane through bridging the three peripheral Gd³⁺ atoms to the central one, while the other Ni(pao)₃⁻ building block (with the Ni2 atom) connects only two terminal Gd³⁺ atoms (Gd2 and Gd4) with the centered Gd1 atom. The formed trigonal bipyramid topology is reminiscent of that of Mn{Mn(hfac)₂}₃{Ni(pao)₃}₂,^{14a} where the Ni(pao)₃⁻ building blocks at two apical sites link to the [Mn₄] triangle plane from the above and below two directions. Furthermore, there are strong hydrogen bonds between the solvent methanol molecule and the coordinated methanol molecule (O28...O27 = 2.608 Å) and between the solvent methanol molecule

and the oximate oxygen atom O3 from the Ni(pao)₃⁻ building block with the Ni1 atom (O28...O3 = 2.621 Å), which are propitious to stabilize the whole crystal structure.

Interestingly, although the cell parameters of complex **2** is quite similar to those of **1**, and both complexes possess the same trigonal bipyramid metal skeleton, there are some subtle structure differences between **1** and **2** worthy to be mentioned. As shown in Fig. 2, the centered Dy1 atom in the [Dy₄] triangle plane of **2** exhibits the same monocapped square-antiprism configuration as the Gd1 atom in **1** (Fig. S2), however, there are three types of peripheral Dy³⁺ ions based on the coordination modes: the Dy2 atom has a monocapped square-antiprism environment similar to that of the Gd2 atom in **1** (Fig. S2), and the Dy3 atom displays a distorted square-antiprism coordinate geometry corresponding to that for the Gd3 atom in **1** (Fig. S2); while the Dy4 atom is eight-coordinate rather than nine-coordinate (Fig. S2), bonded by six oxygen atoms from three hfac⁻ ligands, and two oximate oxygen atoms from two Ni(pao)₃⁻ building blocks, exhibiting a heavily distorted square-antiprism environment, which is obviously different from the monocapped square-antiprism environment of Gd4 atom in **1**. In addition, both complexes have the η²:η²:μ₄-AcO⁻ ligand bridging the Ln2, Ln1 and Ln3 atoms (Ln = Gd and Dy for **1** and **2**, respectively), however, complex **1** possesses the η¹:η²:μ₃-AcO⁻ ligand that connects with the Gd4, Gd1 and Gd3 atoms, whereas the corresponding AcO⁻ ligand in complex **2** only links to the Dy1 and Dy2 atoms using the η¹:η¹:μ₂-bridging mode.

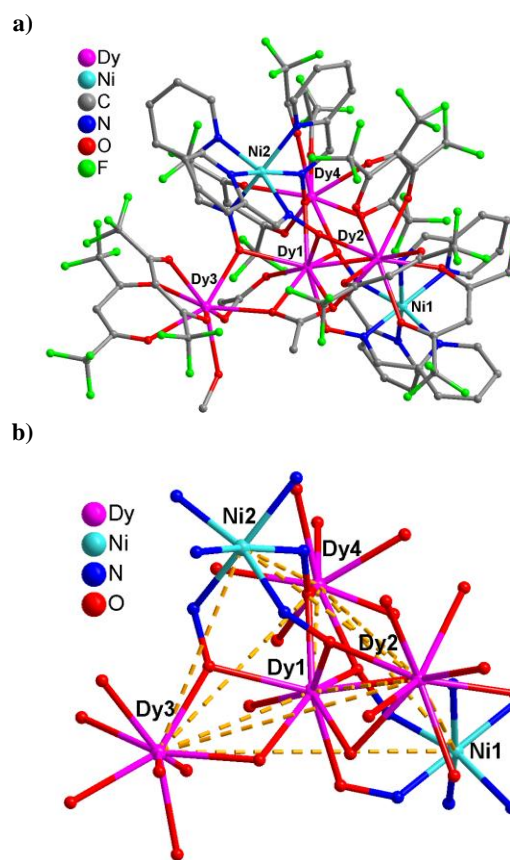


Fig. 2. Crystal structure of **2**, all H atoms and solvent molecules are omitted for clarity (a), and the coordination environments of the Dy and Ni atoms, the dotted lines show the trigonal bipyramid metal topology (b).

The coordinating and bridging modes of the $\text{Ni}(\text{pao})_3^-$ building blocks in **2** are the same as those in **1**, which make these two compounds to have the same trigonal bipyramid metal topology. Furthermore, similar strong hydrogen bonds ($\text{O}28\cdots\text{O}27 = 2.646 \text{ \AA}$ and $\text{O}28\cdots\text{O}3 = 2.639 \text{ \AA}$) are observed for **2**. The Dy-O bond distances of the eight-coordinate Dy atoms (average value of 2.364 and 2.366 \AA for the Dy3 and Dy4 atoms, respectively) are also obviously smaller than those for the nine-coordinate Dy atoms (mean values of 2.445 and 2.410 \AA for the Dy1 and Dy2 atoms, respectively). It is noteworthy that the Dy-O bond lengths of **2** are a little smaller than the corresponding Gd-O bond distances in **1**, as expected, which is ascribed to the radius contraction from the Gd^{3+} ion to the Dy^{3+} ion.

Magnetic properties

The magnetic properties of **1** were investigated as a function of field and temperature, as shown in Fig. 3a, the χT value at room temperature is $34.26 \text{ cm}^3 \cdot \text{K} \cdot \text{mol}^{-1}$, slightly larger than that expected value ($33.5 \text{ cm}^3 \cdot \text{K} \cdot \text{mol}^{-1}$) for two Ni^{2+} ($S = 1$) and four Gd^{3+} ($S = 7/2$, $L = 0$, $^8S_{7/2}$) non-coupling ions (assuming $g_{\text{Gd}} = g_{\text{Ni}} = 2.0$). The χT product increases gradually as the temperature is reduced, then rises sharply when the temperature is lower than 25 K, and finally reaches the largest value of $45.20 \text{ cm}^3 \cdot \text{K} \cdot \text{mol}^{-1}$ at 2 K, suggesting weak ferromagnetic interactions among the metal ions. The magnetic susceptibility data were analyzed by the Curie-Weiss law, extracting the Curie constants (C) of $34.21 \text{ cm}^3 \cdot \text{K} \cdot \text{mol}^{-1}$ and the Weiss constants (θ) of 1.31 K. The small positive θ value validates the weak ferromagnetic interaction.

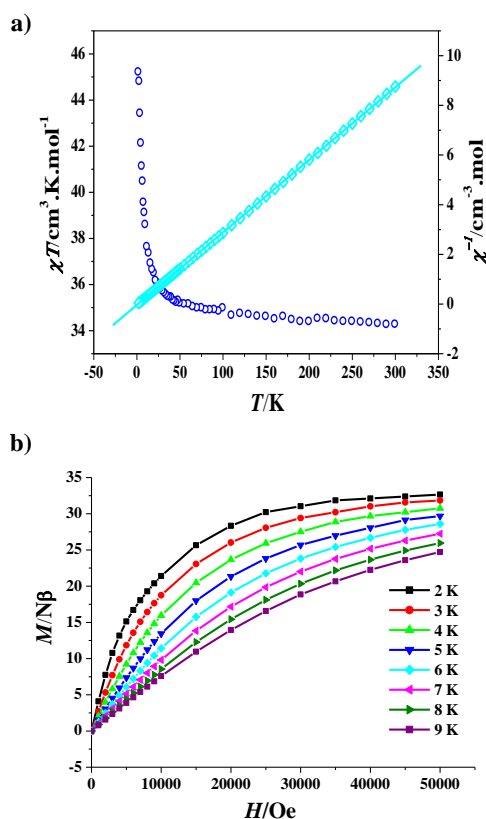


Fig. 3. Plots of χT versus T (\circ) and $1/\chi$ versus T (\diamond) of complex **1**, the solid line represents the best theoretical fitting (a). Isothermal field-dependent curves in the range $T = 2-9 \text{ K}$ for **1** (b).

It is well known that the ferromagnetic coupling among the metal ions brings to a large spin ground state S , which may induce the large magnetic entropy change $\{-\Delta S_m = R \ln(2S+1)\}^{15}$ and the corresponding large MCE. Therefore, the field (H) dependence of the magnetizations (M) of **1** was measured at low temperatures (2-9 K) (Fig. 3b). Under the 50 kOe magnetic field, the magnetization ($32.66 N\beta$) at 2 K is slightly larger than the saturation value of $32 N\beta$ expected for an $S = 16$ system ($g = 2$), further confirming the ferromagnetic interaction. Furthermore, the magnetization slowly increases to reach the saturation value as the field enhances, which indicates that the population of low-lying levels possesses a small magnetic moment only becomes depopulated after employing a large field.^{4f} To examine the magnetic anisotropy, the magnetization ($M/N\beta$) versus H/T curves were reduced, in which the isofield lines are almost superimposed (Fig. 4a), suggesting the weak magnetic anisotropy, which favors the MCE.

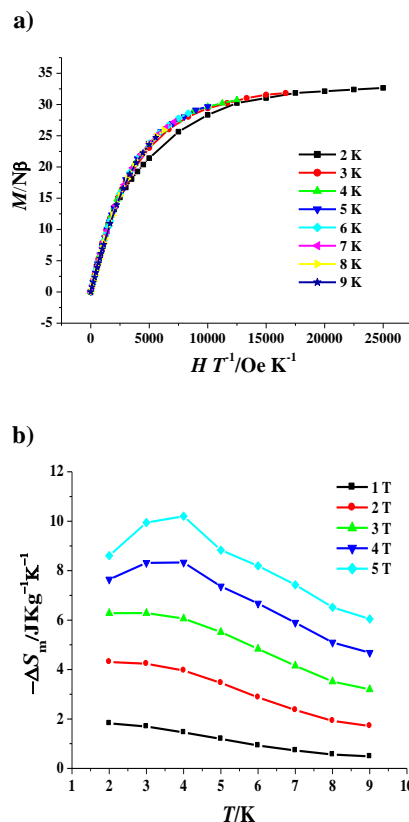


Fig. 4. Plots of reduced magnetization (M) versus H/T for **1** (a). Magnetic entropy change ($-\Delta S_m$) versus T of **1** for applied field changes ΔH (b).

The Maxwell relation $\Delta S_m(T)_{\Delta H} = \int [\partial M(T, H) / \partial T]_H dH$ was adopted to calculate the magnetic entropy changes $-\Delta S_m$.¹⁶ The results are shown in Fig. 4b in the $-\Delta S_m$ versus T curve formation. Obviously, the stronger is the ΔH applied, the larger is the $-\Delta S_m$ value obtained. Notably, the largest $-\Delta S_m$ value for the accessible maximum ΔH of 50 kOe at 4 K is $10.2 \text{ Jkg}^{-1} \text{K}^{-1}$, which is clearly larger than the theoretical maximum entropy for $S = 16$, i.e. $R \ln(2S+1) = 3.50R = 29.07 \text{ Jmol}^{-1} \text{K}^{-1} = 8.73 \text{ Jkg}^{-1} \text{K}^{-1}$. This means the MCE is enhanced, which maybe originates from the presence of low-lying excited S states

thermally accessible even at very low temperatures, such excited states result in an excess of magnetic entropy.^{4a,4c,4e,4f} To the best of our knowledge, only limited manganese, iron and Mn-Gd cluster complexes have been observed to show the enhanced MCE by the Brechin, Dalgarno, Evangelisti, and McInnes groups.^{4a,4c,4e,4f} Although many Ni-Ln heterometallic clusters have been reported to exhibit the MCE,⁵ their largest $-\Delta S_m$ values at 50 kOe are all smaller than or close to the theoretical value calculated by the equation $R\ln(2S+1)$, so complex **1** is the first Ni-Ln cluster complex with the remarkably enhanced MCE. Furthermore, the maximum entropy of **1** is larger than the highest values of some gadolinium-containing intermetallic compounds, for instances, Gd_7Pd_3 ^{17a} and $\text{Gd}_{12}\text{Co}_7$,^{17b} complex **1** is thus a good candidate for the cryogenic magnetic refrigeration materials.

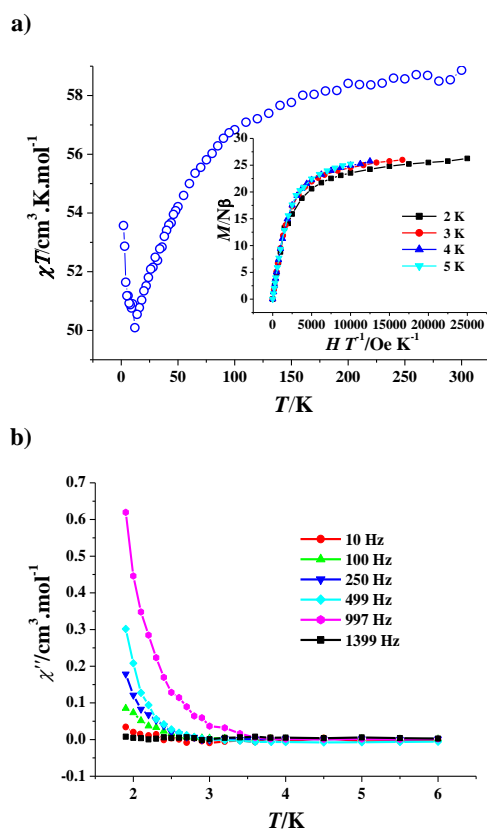


Fig. 5. Plot of χT versus T measured under 1 kOe of **2**. Inset: plots of reduced magnetization (M) versus H/T for **2** (a); temperature dependence of the χ'' component of the ac susceptibility for **2** under a zero dc field (b).

The magnetic behaviours of **2** seem to be quite different from those of **1**. As depicted in Fig. 5a, the room temperature χT value of $58.86 \text{ cm}^3 \cdot \text{K} \cdot \text{mol}^{-1}$ accords with the theory value of $58.68 \text{ cm}^3 \cdot \text{K} \cdot \text{mol}^{-1}$ expected for a non-interacting Ni_2Dy_4 unit (assuming $g_{\text{Ni}} = 2.0$). It decreases continuously with lowering temperature, reaching a minimum value of $50.09 \text{ cm}^3 \cdot \text{K} \cdot \text{mol}^{-1}$ at 12 K, mainly due to the crystal-field effects (thermal depopulation of the Dy^{3+} Stark sublevels). Below this temperature, the χT product abruptly increases to reach $53.57 \text{ cm}^3 \cdot \text{K} \cdot \text{mol}^{-1}$ at 2 K, suggesting the existence of ferromagnetic interactions among the metal ions, as seen for **1**. Therefore, it is

not always credible to judge the nature of the magnetic exchange interaction just according to the temperature dependence of the χT product for the Dy(III)-based complexes. The comparison of the magnetic interactions between **1** and **2** may ascertain the ferromagnetic interactions for **2** at last. Such a method is feasible and has been adopted by several groups to assume the ferromagnetic interactions between the 3d metal ion (Ni^{2+} and Co^{2+}) and the lanthanide ion (Tb^{3+} , Dy^{3+} and Ho^{3+}).^{5i,18}

The field dependence of the magnetization at 2-5 K revealed a rapid increase of magnetization at low magnetic fields, which is in agreement with a high-spin state of ferromagnetic interactions. However, no sign of saturation could be reached owing to the crystal-field splitting of the ground multiplet of the Dy^{3+} ion. The M versus H/T curves are not superimposed (Fig. 5a, inset), suggesting the significant magnetic anisotropy and/or low-lying excited states, required for a SMM. Therefore, alternating-current (ac) magnetic susceptibility measurements were carried out under a 2.5 Oe oscillating field to investigate the dynamics of magnetization. When the dc field was zero, the out-of-phase signals of complex **2** are frequency-dependent, indicating slow relaxation of the magnetization (Fig. 5b). However, net maxima of the χ'' signals were not observed even at frequencies as high as 1400 Hz. One possible reason is the existence of fast quantum tunneling effects. Nevertheless, after applying a dc field of 2000 Oe to fully or partly suppress the quantum tunneling effects, the χ'' signals are still not significantly improved, indicating that quenching of the quantum tunneling effects by this dc field can be negligible. Such a phenomenon was also observed in the other Dy-containing SMMs before.^{5i,19} In addition, the M versus H plot measured at 1.9 K does not show any hysteresis (Fig. S3).

Conclusions

In summary, this work describes two novel ferromagnetic hexanuclear 3d-4f cluster complexes. They have the same 'trigonal bipyramid' metal topology, but one peripheral Ln^{3+} ion of them shows subtle differences on the coordination geometry. Two types of magnetic properties were observed for them, mainly dependent on the lanthanide ions. The $[\text{Ni}_2\text{Gd}_4]$ cluster shows an enhanced MCE mainly due to an excess of entropy change supplied by the low-lying excited S states. Such an enhanced MCE is a rare observation for the cluster complexes. On the other hand, the $[\text{Ni}_2\text{Gd}_4]$ complex displays slow magnetic relaxation of the SMM mainly owing to the large magnetic anisotropy of the Dy^{3+} ion.

Acknowledgements

This work was supported by National Key Basic Research Program of China (2013CB933403), National Natural Science Foundation of China (21073198 and 91022014), and the Strategic Priority Research Program of the Chinese Academy of Sciences (XDB12010103).

Notes and references

^a Beijing National Laboratory for Molecular Sciences, Center for Molecular Science, Institute of Chemistry, Chinese Academy of Sciences, Beijing 100190, P. R. China; E-mail: cmliu@iccas.ac.cn

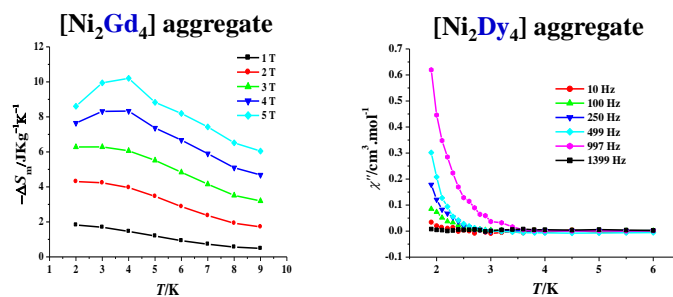
† Footnotes should appear here. These might include comments relevant to but not central to the matter under discussion, limited experimental and spectral data, and crystallographic data.

Electronic Supplementary Information (ESI) available: Additional figures of the crystal structure (Fig. S1 and S2) and magnetic

characterization (Fig. S3). CCDC reference numbers 1016867-1016868. For crystallographic data in CIF or other electronic format see DOI: 10.1039/b000000x/

- 1 C. Benelli and D. Gatteschi, *Chem. Rev.*, 2002, **102**, 2369.
- 2 Y.-Z. Zheng, G.-J. Zhou, Z. Zheng and R. E. P. Winpenny, *Chem. Soc. Rev.*, 2014, **43**, 1462.
- 3 (a) R. Sessoli, D. Gatteschi, A. Caneschi and M. A. Novak, *Nature*, 1993, **365**, 141; (b) G. Christou, D. Gatteschi, D. N. Hendrickson and R. Sessoli, *MRS Bull.*, 2000, **25**, 66; (c) D. Gatteschi and R. Sessoli, *Angew. Chem. Int. Ed.*, 2003, **42**, 268; (d) G. Aromi and E. K. Brechin, *Struct. Bonding*, 2006, **122**, 1; (e) L. M. C. Beltran and J. R. Long, *Acc. Chem. Res.*, 2005, **38**, 325; (f) R. Bagai and G. Christou, *Chem. Soc. Rev.*, 2009, **38**, 1011; (g) V. Chandrasekhar and B. Murugesapandian, *Acc. Chem. Res.*, 2009, **42**, 1047; (h) R. Sessoli, and A. K. Powell, *Coord. Chem. Rev.*, 2009, **253**, 2328; (i) G. E. Kostakis, A. M. Akoab and A. K. Powell, *Chem. Soc. Rev.*, 2010, **39**, 2238; (j) M. Murrie, *Chem. Soc. Rev.*, 2010, **39**, 1986; (k) D. N. Woodruff, R. E. P. Winpenny and R. A. Layfield, *Chem. Rev.*, 2013, **113**, 5110; (l) B.-W. Wang, X.-Y. Wang, H.-L. Sun, S.-D. Jiang and S. Gao, *Phil. Trans. R. Soc. A.*, 2013, **371**, 20120316; (m) T. Komeda, H. Isshiki, J. Liu, Y.-F. Zhang, N. Lorente, K. Katoh, B. K. Breedlove and M. Yamashita, *Nat. Comm.*, 2011, **2**, 217; (n) R. Vincent, S. Klyatskaya, M. Ruben, W. Wernsdorfer and F. Balestro, *Nature*, 2012, **488**, 357.
- 4 (a) M. Evangelisti, A. Candini, A. Ghirri, M. Affronte, E. K. Brechin and E. J. L. McInnes, *Appl. Phys. Lett.*, 2005, **87**, 072504; (b) M. Evangelisti, F. Luis, L. J. de Jongh and M. Affronte, *J. Mater. Chem.*, 2006, **16**, 2534; (c) R. Shaw, R. H. Laye, L. F. Jones, D. M. Low, C. Talbot-Eeckelaers, Q. Wei, C. J. Milios, S. Teat, M. Helliwell, J. Raftery, M. Evangelisti, M. Affronte, D. Collison, E. K. Brechin and E. J. L. McInnes, *Inorg. Chem.*, 2007, **46**, 4968; (d) M. Manoli, R. D. L. Johnstone, S. Parsons, M. Murrie, M. Affronte, M. Evangelisti and E. K. Brechin, *Angew. Chem. Int. Ed.*, 2007, **46**, 4456; (e) M. Manoli, A. Collins, S. Parsons, A. Candini, M. Evangelisti and E. K. Brechin, *J. Am. Chem. Soc.*, 2008, **130**, 11129; (f) G. Karotsis, M. Evangelisti, S. J. Dalgarno and E. K. Brechin, *Angew. Chem. Int. Ed.*, 2009, **48**, 9928; (g) S. K. Langley, N. F. Chilton, B. Moubaraki, T. Hooper, E. K. Brechin, M. Evangelisti and K. S. Murray, *Chem. Sci.*, 2011, **2**, 1166; (h) M. Evangelisti, O. Roubeau, E. Palacios, A. Camón, T. N. Hooper, E. K. Brechin and J. J. Alonso, *Angew. Chem. Int. Ed.*, 2011, **50**, 6606; (i) J.-D. Leng, J.-L. Liu and M.-L. Tong, *Chem. Commun.*, 2012, **48**, 5286; (j) Z.-M. Zhang, L.-Y. Pan, W.-Q. Lin, J.-D. Leng, F.-S. Guo, Y.-C. Chen, J.-L. Liu and M.-L. Tong, *Chem. Commun.*, 2013, **49**, 8081; (k) Y.-L. Hou, G. Xiong, P.-F. Shi, R.-R. Cheng, J.-Z. Cui and B. Zhao, *Chem. Commun.*, 2013, **49**, 6066; (l) J.-P. Zhao, R. Zhao, Q. Yang, B.-W. Hu, F.-C. Liu and X.-H. Bu, *Dalton Trans.*, 2013, **42**, 14509; (m) G. Xiong, H. Xu, J.-Z. Cui, Q.-L. Wang and B. Zhao, *Dalton Trans.*, 2014, **43**, 5639; (n) K. S. Pedersen, G. Lorusso, J. J. Morales, T. Weyhermüller, S. Piligkos, S. K. Singh, D. Larsen, M. Schaub-Magnussen, G. Rajaraman, M. Evangelisti and J. Bendix, *Angew. Chem. Int. Ed.*, 2014, **53**, 2394; (o) I. Kornarakis, G. Sopsis, C. J. Milios and G. S. Armatas, *RSC Adv.*, 2012, **2**, 9809.
- 5 (a) Y. Z. Zheng, M. Evangelisti and R. E. Winpenny, *Angew. Chem. Int. Ed.*, 2011, **50**, 3692; (b) J. B. Peng, Q. C. Zhang, X. J. Kong, Y. P. Ren, L. S. Long, R. B. Huang, L. S. Zheng and Z. Zheng, *Angew. Chem. Int. Ed.*, 2011, **50**, 10649; (c) J. B. Peng, Q. C. Zhang, X. J. Kong, Y. Z. Zheng, Y. P. Ren, L. S. Long, R. B. Huang, L. S. Zheng and Z. Zheng, *J. Am. Chem. Soc.*, 2012, **134**, 3314; (d) T. N. Hooper, J. Schnack, S. Piligkos, M. Evangelisti and E. K. Brechin, *Angew. Chem. Int. Ed.*, 2012, **51**, 4633; (e) Z. Y. Li, J. Zhu, X. Q. Wang, J. Ni, J. J. Zhang, S. Q. Liu and C. Y. Duan, *Dalton Trans.*, 2013, **42**, 5711; (f) J. W. Sharples and D. Collison, *Polyhedron*, 2013, **54**, 91; (g) P. Wang, S. Shannigrahi, N. L. Yakovlev and T. S. Andy Hor, *Dalton Trans.*, 2014, **43**, 182; (h) T. D. Pasatou, A. Ghirri, A. M. Madalan, M. Affronte and M. Andruh, *Dalton Trans.*, 2014, **43**, 9136; (i) S. Das, A. Dey, S. Kundu, S. Biswas, A. J. Mota, E. Colacio and V. Chandrasekhar, *Chem.-Asian J.*, 2014, **7**, 1876; (j) A. Upadhyay, N. Komatireddy, A. Ghirri, F. Tuna, S. K. Langley, A. K. Srivastava, E. C. Sañudo, B. Moubaraki, K. S. Murray, E. J. L. McInnes, M. Affronte and M. Shanmugam, *Dalton Trans.*, 2014, **43**, 259.
- 6 (a) C.-M. Liu, D.-Q. Zhang, X. Hao and D.-B. Zhu, *Cryst. Growth & Des.*, 2012, **12**, 2948; (b) C.-M. Liu, D.-Q. Zhang and D. B. Zhu, *Inorg. Chem.*, 2013, **52**, 8933; (c) C.-M. Liu, D.-Q. Zhang and D. B. Zhu, *Dalton Trans.*, 2013, **42**, 14813; (d) C.-M. Liu, D.-Q. Zhang, X. Hao and D.-B. Zhu, *Chem.-Asian J.*, 2014, **7**, 1841; (e) C.-M. Liu, D.-Q. Zhang and D. B. Zhu, *RSC Adv.*, 2014, **4**, 36053.
- 7 C.-M. Liu, D.-Q. Zhang and D. B. Zhu, *Dalton Trans.*, 2010, **39**, 11325.
- 8 R. A. Krause and D. H. Busch, *J. Am. Chem. Soc.*, 1960, **82**, 4830.
- 9 (a) H.-B. Xu, J. Li, L.-Y. Zhang, X. Huang, B. Li and Z.-N. Chen, *Cryst. Growth & Des.*, 2010, **10**, 4101; (b) H.-B. Xu, Y.-T. Zhong, W.-X. Zhang, Z.-N. Chen and X.-M. Chen, *Dalton Trans.*, 2010, **39**, 5676.
- 10 O. Kahn, *Molecular Magnetism*, VCH, New York, 1993.
- 11 (a) G. M. Sheldrick, SHELXS 97, Program for the Solution of Crystal Structures, University of Göttingen, Göttingen, Germany, 1997; (b) G. M. Sheldrick, SHELXL 97, Program for the Refinement of Crystal Structures, University of Göttingen, Göttingen, Germany, 1997.
- 12 For examples: (a) C. J. Milios, A. Vinslava, P. A. Wood, S. Parsons, W. Wernsdorfer, G. Christou, S. P. Perlepes and E. K. Brechin, *J. Am. Chem. Soc.*, 2007, **129**, 8; (b) C.-I. Yang, W. Wernsdorfer, G.-H. Lee and H.-L. Tsai, *J. Am. Chem. Soc.*, 2007, **129**, 456; (c) C. J. Milios, A. Vinslava, S. Moggach, S. Parsons, W. Wernsdorfer, G. Christou, S. P. Perlepes and E. K. Brechin, *J. Am. Chem. Soc.*, 2007, **129**, 2754; (d) C. J. Milios, R. Inglis, A. Vinslava, R. Bagai, W. Wernsdorfer, S. Parsons, S. P. Perlepes, G. Christou and E. K. Brechin, *J. Am. Chem. Soc.*, 2007, **129**, 12505; (e) C. J. Milios, R. Inglis, R. Bagai, W. Wernsdorfer, A. Collins, S. Moggach, S. Parsons, S. P. Perlepes, G. Christou and E. K. Brechin, *Chem. Commun.*, 2007, 3476; (f) C. C. Stoumpos, R. Inglis, O. Roubeau, H. Sartz, A. A. Kitos, C. J. Milios, G. Aromi, A. J. Tasiopoulos, V. Nastopoulos, E. K. Brechin and S. P. Perlepes, *Inorg. Chem.*, 2010, **49**, 4388.
- 13 C. Papatriantafyllou, T. C. Stamatas, C. G. Eftymiou, L. Cunha-Silva, F. A. A. Paz, S. P. Perlepes and G. Christou, *Inorg. Chem.*, 2010, **49**, 9743.
- 14 (a) H. Miyasaka, T. Nezu, F. Iwahori, S. Furukawa, K. Sugimoto, R. Cléac, K.-i. Sugiura and M. Yamashita, *Inorg. Chem.*, 2003, **42**, 4501; (b) H. Chen, C.-B. Ma, D.-Q. Yuan, M.-Q. Hu, H.-M. Wen, Q.-T. Liu and C.-N. Chen, *Inorg. Chem.*, 2011, **50**, 10342.
- 15 M. Evangelisti and E. K. Brechin, *Dalton Trans.*, 2010, **39**, 4672.
- 16 V. K. Pecharsky and K. A. Gschneidner, Jr., *J. Magn. Magn. Mater.*, 1999, **200**, 44.
- 17 (a) F. Canepa, M. Napoletano and S. Cirafici, *Intermetallics*, 2002, **10**, 731; (b) X. Chen and Y. H. Zhuang, *Solid State Commun.*, 2008, **148**, 322.
- 18 (a) V. Chandrasekhar, B. M. Pandian, R. Azhakar, J. J. Vittal and R. Cléac, *Inorg. Chem.*, 2007, **46**, 5140; (b) V. Chandrasekhar, B. M. Pandian, J. J. Vittal and R. Cléac, *Inorg. Chem.*, 2009, **48**, 1148; (c) T. Yamaguchi, J. P. Costes, Y. Kishima, M. Kojima, Y. Sunatsuki, N. Brefuel, J. P. Tuchagues, L. Vendier and W. Wernsdorfer, *Inorg. Chem.*, 2010, **49**, 9125; (d) E. Colacio, J. Ruiz, A. J. Mota, M. A. Palacios, E. Cremades, E. Ruiz, F. J. White and E. K. Brechin, *Inorg. Chem.*, 2012, **51**, 5857; (e) M. Towatari, K. Nishi, T. Fujinami, N. Matsumoto, Y. Sunatsuki, M. Kojima, N. Mochida, T. Ishida, N. Re and J. Mrozinski, *Inorg. Chem.*, 2013, **52**, 6160.
- 19 S. Titos-Padilla, J. Ruiz, J. M. Herrera, E. K. Brechin, W. Wernsdorfer, F. Lloret and E. Colacio, *Inorg. Chem.*, 2013, **52**, 9620.

Graphical Abstract



Two hexanuclear $[\text{Ni}_2\text{Ln}_4]$ aggregates exhibit either an enhanced magnetocaloric effect or slow magnetic relaxation, depending on the lanthanide ions chose.